Title	Preparation of Preyssler-type Phosphotungstate with One Central Potassium Cation and Potassium Cation Migration into the Preyssler Molecule to form Di-Potassium-Encapsulated Derivative
Auther(s)	Hayashi, Akio; Nur Khoiru Wihadi, Muh; Ota, Hiromi; Xavier, Lo´pez; Ichihashi, Katsuya; Nishihara, Sadafumi; Inoue, Katsuya; Tsunoji, Nao; Sano, Tsuneji; Sadakane, Masahiro
Citation	ACS Omega , 3 (2) : 2363 - 2373
Issue Date	2018-02-27
DOI	10.1021/acsomega.8b00163
Self DOI	
URL	http://ir.lib.hiroshima-u.ac.jp/00046761
Right	Copyright © 2018 American Chemical Society, This is an open access article published under an ACS AuthorChoice License, which permits copying and redistribution of the article or any adaptations for non-commercial purposes.
Relation	

ACS OMEGA

Article

Cite This: ACS Omega 2018, 3, 2363−2373

Preparation of Preyssler-type Phosphotungstate with One Central Potassium Cation and Potassium Cation Migration into the Preyssler Molecule to form Di-Potassium-Encapsulated Derivative

Akio Hayashi,[†] Muh. Nur Khoiru Wihadi,[†] Hiromi Ota,[‡] Xavier López,[§] Katsuya Ichihashi,[∥] Sadafumi Nishihara,[∥,⊥,#] Katsuya Inoue,[∥,⊥,#] Nao Tsunoji,[†] Tsuneji Sano,[†] and Masahiro Sadakane*[,†]

[†]Department of Applied Chemistry, Graduate School of Engineering, Hiroshima University, 1-4-1 Kagamiyama, Higashi-Hiroshima 739-8527, Japan

[‡]Division of Instrumental Analysis, Department of Instrumental Analysis and Cryogenics, Advanced Science Research Center, Okayama University, 3-1-1 Tsushima-Naka, Kita-ku, Okayama 700-8530, Japan

[§]Departament de Química Física i Inorgànica, Universitat Rovira i Virgili, c/Marcel·lí Domingo 1, 43007 Tarragona, Spain

[∥]Graduate School of Science, [⊥]Chirality Research Center, and [#]Institute for Advanced Materials Research, Hiroshima University, 1-3-1 Kagamiyama, Higashi-Hiroshima 739-8526, Japan

Supporting Information

ABSTRACT: A mono-potassium cation-encapsulated Preyssler-type phosphotungstate, $[P_5W_{30}O_{110}K]^{14-}$ (**1**), was prepared as a potassium salt, $K_{14}[P_5W_{30}O_{110}K]$ (**1a**), by heating mono-bismuth- or mono-calcium-encapsulated Preyssler-type phosphotungstates ($K_{12}[P_5W_{30}O_{110}Bi(H_2O)]$ or $K_{13}[P_5W_{30}O_{110}Ca(H_2O)]$) in acetate buffer. Characterization of the potassium salt **1a** by single-crystal X-ray structure analysis, ^{31}P and ^{183}W nuclear magnetic resonance (NMR) spectroscopy, Fourier transform infrared spectroscopy, high-resolution electrospray ionization mass spectroscopy, and elemental analysis revealed that one potassium cation is encapsulated in the central cavity of the Preyssler-type phosphotungstate molecule with a formal D_{5h} symmetry. Density functional theory calculations have confirmed that the potassium cation prefers the central position of the cavity over a side position, in which no water molecules are coordinated to the encapsulated potassium cation. ^{31}P NMR and cyclic voltammetry analyses revealed the rapid protonation−deprotonation of the oxygens in the cavity compared to that of other Preyssler-type compounds. Heating of **1a** in the solid state afforded a di-K^+-encapsulated compound, $K_{13}[P_5W_{30}O_{110}K_2]$ (**2a**), indicating that a potassium counter-cation is introduced in one of the side cavities, concomitantly displacing the internal potassium ion from the center to a second side cavity, thus providing a new method to encapsulate an additional cation in Preyssler compounds.

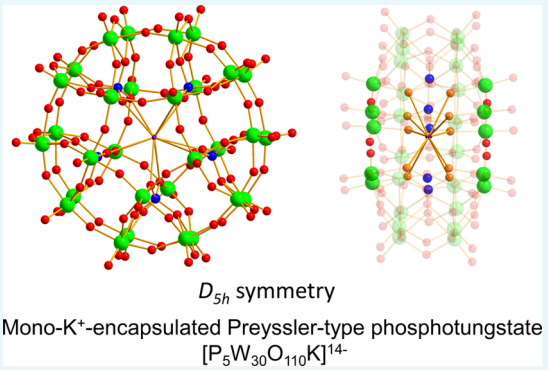

INTRODUCTION

Tungsten forms anionic mixed metal oxides with other cationic elements to afford heteropolytungstates. Such compounds display acidic, multielectron redox, and photochemical properties and have thus attracted increasing interest as catalysts and functional materials.[1−3] Preyssler-type phosphotungstates, $[P_5W_{30}O_{110}M^{n+}(H_2O)]^{(15-n)-}$ (M: encapsulated cation), contain five PO_4 tetrahedra surrounded by 30 WO_6 octahedra (10 cap tungsten and 20 belt tungsten) forming a doughnut-shaped molecule (Figure 1), and have been employed as acid catalysts[4] and functional materials.[5−7] Preyssler compounds can encapsulate different cations (M) such as Na^+,[8,9] Ag^+,[5,10,11] K^+,[12,13] lanthanoid cations,[9,14−18] Ca^{2+},[9,18,19] Bi^{3+},[9,18,20] Y^{3+},[9,18,19] and actinoid metals,[9,14,15,19,21] and their properties such as the redox potentials, magnetic properties, and thermal stability can be tuned by exchanging the encapsulated cations.[9,15,16,18,22−28] Such Preyssler compounds present two types of cavities: (1) one central cavity surrounded by 10 oxygens (O_a) bound to P atoms and (2) two side cavities surrounded by 5 oxygens (O_a) bound to P atoms and 5 bridging oxygens (O_b) between two cap tungsten atoms (Figure 1).

In almost all of the Preyssler-type phosphotungstates, the encapsulated cation occupies one of the two side cavities, presenting a coordination with five O_a oxygens, five O_b oxygens, and one coordinating water molecule (Figure 1c). One exception is the di-K^+-encapsulated Preyssler-type phosphotungstate $[P_5W_{30}O_{110}K_2]^{13-}$ (**2**), which we reported

Received: January 25, 2018
Accepted: February 13, 2018
Published: February 27, 2018

DOI: 10.1021/acsomega.8b00163
ACS Omega 2018, 3, 2363−2373

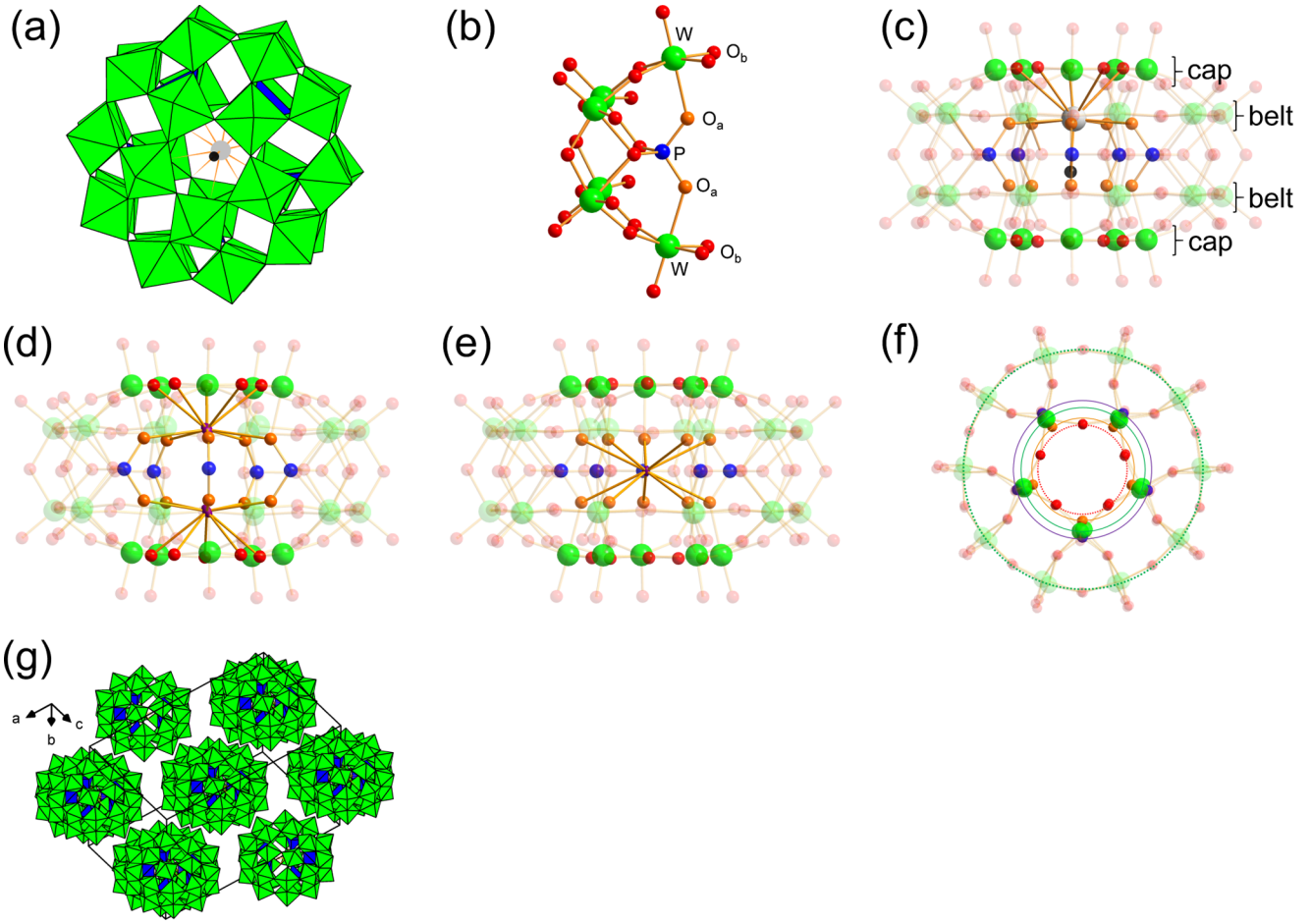

Figure 1. (a) Polyhedral representation of a Preyssler-type phosphotungstate molecule with one encapsulated cation. (b) Ball-and-stick representation of one-fifth of the Preyssler-type phosphotungstate $[PW_6O_{22}]$ unit. Ball-and-stick representation of a (c) mono-cation-encapsulated Preyssler-type molecule, (d) di-K^+-encapsulated Preyssler-type molecule **2**, (e) mono-K^+-encapsulated Preyssler-type molecule **1**, and (f) concentric circles on the oxygen, tungsten, and phosphorus atoms. (g) Polyhedral presentation of the packing of $K_{14}[P_5W_{30}O_{110}K]\cdot nH_2O$ (**1a**) in the unit cell. Green, blue, red, orange, gray, black, and violet balls indicate tungsten, phosphorus, oxygen, oxygen surrounding the central cavity, mono-encapsulated cation, water molecule oxygen coordinated to the cation, and potassium atoms, respectively.

in a previous paper.[29] In this compound, two potassium cations are located in the side cavities (Figure 1d). Wang's group reported a K^+ located in the central cavity of a Preyssler-type sulfotungstate, $[S_5W_{30}O_{110}K]^{9-}$, where K^+ was coordinated by 10 O_a oxygens (Figure 1e).[30]

In this paper, we report a new Preyssler-type phosphotungstate with one encapsulated potassium cation in the central cavity, $[P_5W_{30}O_{110}K]^{14-}$ (**1**) (Figure 1e), and the migration of a potassium counter-cation into the molecule in the solid state to form a di-K^+ species (**2**).

RESULTS AND DISCUSSION

Preparation and Isolation of $K_{14}[P_5W_{30}O_{110}K]$ (1a). $K_{13}[P_5W_{30}O_{110}Ca(H_2O)]$ was dissolved in a potassium acetate buffer (pH 4.7) in the presence of KCl and heated at 170 °C for 24 h (Table 1, entry 4). Once the reaction mixture had cooled down to room temperature, a colorless solid was obtained. The ^{31}P NMR spectrum of the solid shows three singlets at −8.96, −10.15, and −10.96 ppm (Figure 2b); the peaks at −8.96 and −10.96 ppm were assigned to the starting material, $[P_5W_{30}O_{110}Ca(H_2O)]^{13-}$, and the di-$K^+$-encapsulated derivative, $[P_5W_{30}O_{110}K_2]^{13-}$ (**2**), respectively. The peak at −10.15 ppm is not assignable to any known species. The ^{31}P NMR spectrum of the filtrate shows two singlets at 0.75 and −11.47 ppm (Figure 2c), where the singlet at 0.75 ppm may correspond to phosphate species and the singlet at −11.47 ppm is not assignable. Repeated recrystallization of the solid from hot water afforded colorless crystals showing only the ^{31}P NMR singlet at −10.15 ppm (Figure 2e,f).

Single-Crystal Structure Analysis of $K_{14}[P_5W_{30}O_{110}K]$. The single-crystal structure analysis revealed that the isolated colorless crystals belong to a Preyssler-type phosphotungstate with one encapsulated potassium cation (K^+) (Figure 1e). The potassium cation is located in the central cavity on a pseudo-fivefold rotation axis of the molecule coordinated by 10 P−O_a oxygens with bond distances of 2.934−2.962 Å. No water molecules coordinating the central K^+ ion were found.

A few reports on mono-K^+-encapsulated Preyssler-type compounds have been published. Sun's group reported Preyssler-type phosphotungstates, where one K^+ was placed in one of the side cavities with a coordinated water molecule. On the other hand, Wang's group reported a Preyssler-type sulfotungstate, where a K^+ ion was placed in the central cavity. $K_{14}[P_5W_{30}O_{110}K]$ (**1a**) is the first example in which a K^+ ion is placed in the central cavity of a Preyssler-type phosphotungstate. Similar to the potassium salt of the di-K^+-encapsulated Preyssler compound, $K_{13}[P_5W_{30}O_{110}K_2]$ (**2a**),[29] **1a** crystallizes in an orthorhombic space group (Figure 1g), where counter-

DOI: 10.1021/acsomega.8b00163
ACS Omega 2018, 3, 2363−2373

Table 1. Yield of Mono-K- and Di-K-Encapsulated Preyssler-type Phosphotungstates under Different Conditions

	reaction conditions			yield[a]		
entry	solution[b]	added KCl	temp. time	$[P_5W_{30}O_{110}K]^{14-}$ (**1**)	$[P_5W_{30}O_{110}K_2]^{13-}$ (**2**)	recov.[a]
			Starting Compound: $K_{13}[P_5W_{30}O_{110}Ca(H_2O)]$ (0.3 mmol)			
1	1 M KOAc	0 mmol	170 °C 24 h	11	16	52
2	1 M KOAc	0 mmol	170 °C 48 h	9	44	36
3	1 M KOAc	3 mmol	170 °C 24 h	14	18	48
4	1 M KOAc	6 mmol	170 °C 24 h	15	18	35
5	1 M KOAc	6 mmol	170 °C 48 h	1	61	2
6	1 M KOAc	9 mmol	170 °C 24 h	13	22	29
7	1 M KOAc	18 mmol	170 °C 24 h	8	36	6
8	1 M LiOAc	0 mmol	170 °C 48 h	0	4	33
			Starting Compound: $K_{12}[P_5W_{30}O_{110}Bi(H_2O)]$ (0.3 mmol)			
9	1 M LiOAc	0 mmol	170 °C 24 h	4	28	1
10	1 M KOAc	0 mmol	170 °C 24 h	0	17	59
11	1 M KOAc	5 mmol	170 °C 24 h	0	9	60
12	1 M KOAc	18 mmol	170 °C 24 h	0	49	0
13	1 M KOAc	0 mmol	125 °C 24 h	0	0	no reaction[c]
14	H_2O	5 mmol	170 °C 24 h	0	0	no reaction[c]
15	0.1 M HCl	5 mmol	170 °C 24 h	0	0	no reaction[c]
			Starting Compound: $K_{14}[P_5W_{30}O_{110}Na(H_2O)]$ (0.3 mmol)			
16	1 M KOAc	18 mmol	170 °C 24 h	0	0	no reaction[c]

[a]The solid obtained after cooling down the reaction mixture contained only Preyssler species (starting compound, **1a** and **2a**), and the conversions and yields were estimated based on the ^{31}P NMR integration ratio and the amount of solid isolated. No Preyssler species remained in the solution. [b]pH = 4.7, 5 mL containing 5 mmol of K^+. [c]Only the starting compound was detected in the solid and the solution obtained after the reaction.

cations and solvent molecules are located between the molecules.

A summary of the parameters of the $[P_5W_{30}O_{110}K]^{14-}$ (**1**) unit in **1a** is presented in Table 2, together with those of the $[P_5W_{30}O_{110}K_2]^{13-}$ (**2**) unit in **2a**. The molecular size is quite similar, although the diameter of the circle going through the five O_a atoms in **1** is slightly larger than that in **2**.

IR, Elemental Analysis, High-Resolution Electrospray Ionization Mass Spectroscopy (HR-ESI-MS), and ^{183}W NMR Analysis of $K_{14}[P_5W_{30}O_{110}K]$ (1a). The IR spectrum of **1a** shows the characteristic bands of a Preyssler-type phosphotungstate at 1173, 1088, 1012, 985, 930, 906, and 794 cm^{-1} (Figure 3b), similar to those of mono-$Na^+(H_2O)$-encapsulated Preyssler-type phosphotungstates (Figure 3a) and **2a** (Figure 3d), but with some bands slightly shifted (Table 2). We have previously reported that the IR bands of **2** are sharper than those of mono-$Na^+(H_2O)$-encapsulated compounds because the higher symmetry of the di-K^+ compound (D_{5h}) gives fewer peaks with more degenerate normal modes of vibration than those of the $Na^+(H_2O)$ compound (C_{5v}).[29] The IR bands of **1a** are also sharper than those of $Na^+(H_2O)$ compounds, confirming that **1a** bears one central K^+ ion with D_{5h} symmetry.

The elemental analysis revealed that the formula of **1a** is $K_{14}[P_5W_{30}O_{110}K]\cdot 26H_2O$. The HR-ESI-MS spectrum of **1a** dissolved in a CH_3CN/H_2O mixture showed the characteristic peaks for $H_8[P_5W_{30}O_{110}K]^{6-}$, $H_9[P_5W_{30}O_{110}K]^{5-}$, $H_{10}[P_5W_{30}O_{110}K]^{6-}$, and their dehydrated species (Figure S1), indicating also the presence of $[P_5W_{30}O_{110}K]^{14-}$ species in the solution.

Figure 4 shows the ^{183}W NMR spectra of **1a**, **2a**, and $K_{14}[P_5W_{30}O_{110}Na(H_2O)]$ dissolved in D_2O. The spectrum of the mono-$Na(H_2O)$-encapsulated Preyssler-type phosphotungstate shows four singlets with a 2:2:1:1 integration ratio (Figure 4c) owing to its C_{5v} symmetry, where the belt and cap tungsten atoms close to the encapsulated Na^+ are not equivalent to those far from the encapsulated cation (Figure 1d). The ^{183}W NMR spectrum of $[P_5W_{30}O_{110}K]^{14-}$ (**1**) displays two singlets at −208.2 and −302.1 ppm with a 2:1 integration ratio (Figure 4a), similar to the ^{183}W NMR spectrum of $[P_5W_{30}O_{110}K_2]^{13-}$

DOI: 10.1021/acsomega.8b00163
ACS Omega 2018, 3, 2363−2373

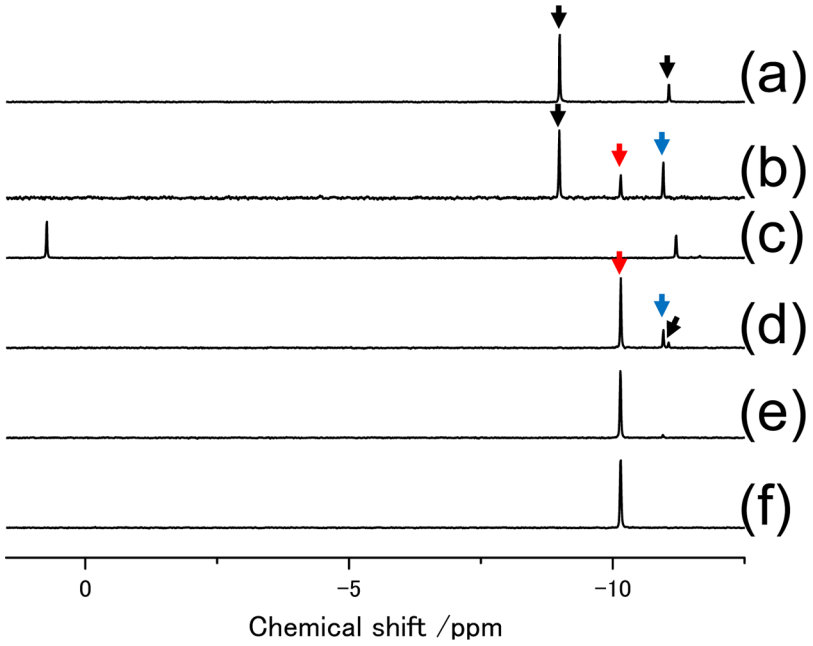

Figure 2. ^{31}P NMR spectra of (a) $[P_5W_{30}O_{110}Ca(H_2O)]^{13-}$, (b) the solid, and (c) solution obtained after the reaction of $K_{13}[P_5W_{30}O_{110}Ca(H_2O)]$ in KOAc buffer (pH 4.7) in the presence of KCl (6 mmol, Table 1, entry 4), and the solid obtained after the (d) first, (e) second, and (f) third recrystallization. The $[P_5W_{30}O_{110}Ca(H_2O)]^{13-}$ spectra display one singlet or two singlets depending on the pH of the solution. The black, blue, and red arrows indicate the signals for $[P_5W_{30}O_{110}Ca(H_2O)]^{13-}$, $[P_5W_{30}O_{110}K_2]^{13-}$, and the new species, respectively. The solid (ca. 50 mg) was dissolved in ca. 1.0 mL of D_2O.

Table 2. Comparison of the NMR Chemical Shift, Infrared (IR) Wavenumber, and Size of the Two Potassium-Encapsulated Preyssler-type Phosphotungstates

	mono-K, $K_{14}[P_5W_{30}O_{110}K]$ (**1a**)	di-K, $K_{13}[P_5W_{30}O_{110}K_2]$ (**2a**)
	NMR Chemical Shift (ppm)	
^{31}P	−10.15	−10.96
^{183}W	−208.2 (20W), −302.1 (10W)	−205.6 (20W), −265.1 (10W)
IR bands (cm^{-1})	1173, 1088, 1012, 985, 930, 906, 794	1178, 1088, 1016, 987, 935, 908, 781
	Diameter (Å) of the Circle Going through the Given Atoms[a]	
O_a	4.5849	4.4874
O_b	5.3456	5.3800
cap W	6.3485	6.3922
P	7.0447	7.0110
belt W	12.2746	12.2818
	Thickness (Å): Distance between Belt or Cap Tungsten Atoms	
belt W	3.3233	3.3251
cap W	6.6959	6.7530

[a]Diameter of the concentric circles for the five O_a, O_b, Cap W, or P atoms (Figure 1f).

(**2**) (Figure 4b) but with different chemical shifts (Table 2). The presence of two singlets in a 2:1 integration ratio indicates that both the cap and belt tungsten atoms are equivalent, suggesting that the isolated Preyssler-type phosphotungstate with one central K^+ is stable in the aqueous solution.

Density Functional Theory (DFT) Calculations. The structure of **1a** differs from that of other Preyssler-type phosphotungstates, in which one cation is encapsulated in the side cavity coordinated by one water molecule. To confidently assign the obtained structure, we calculated the relative stability of all of the possible structures (Table 3). The calculations revealed that the mono-K^+-encapsulated Preyssler structure with a K^+ ion sitting in the central cavity in the absence of water coordination is 35.74 kcal mol^{-1} more stable than that with the cation sitting in one of the side cavities with a coordinated water molecule (entry 1). The mono-K^+-encapsulated Preyssler structure with the K^+ ion in a side cavity without a coordinated water molecule is 20.17 kcal mol^{-1} more stable than that presenting a solvent coordination (entry 2). These results suggest that the coordination of a water molecule is not the preferred situation when K^+ is present inside the Preyssler cluster. Furthermore, the mono-K^+-encapsulated Preyssler without coordinated water is 15.6 kcal mol^{-1} more stable when K^+ is in the central cavity than when it is located in a side cavity (entry 3). These results suggest that a structure with one central K^+ with no water coordination is theoretically reasonable.

In contrast, Sun's group has reported mono-K^+-encapsulated Preyssler-type compounds where one K^+ ion is sitting in one of the side cavities and one water molecule is coordinated to the K^+ in Preyssler-metal−organic hybrid coordination poly-

DOI: 10.1021/acsomega.8b00163
ACS Omega 2018, 3, 2363−2373

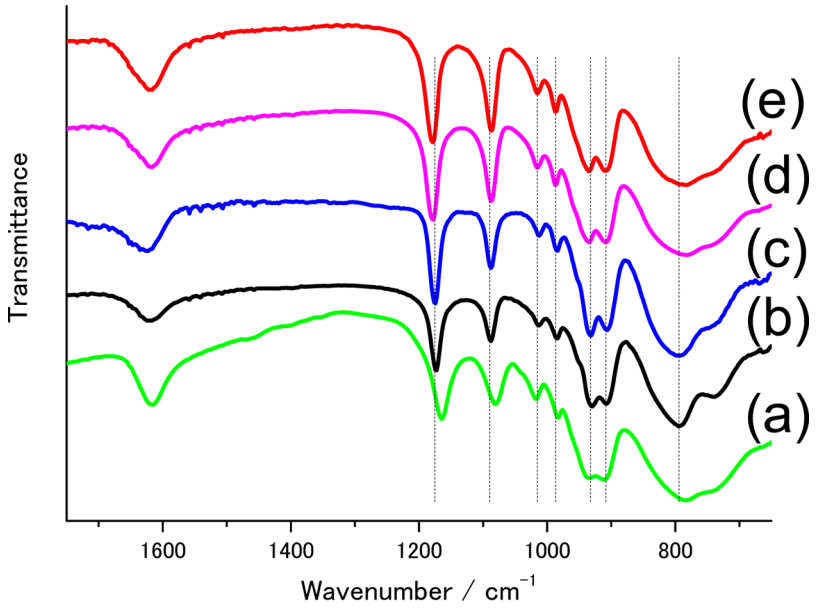

Figure 3. IR spectra of (a) $K_{14}[P_5W_{30}O_{110}Na]$, (b) $K_{14}[P_5W_{30}O_{110}K]$ (**1a**), (c) $H_{14}[P_5W_{30}O_{110}K]$ (**1b**), (d) $K_{13}[P_5W_{30}O_{110}K]$ (**1a**) heated at 300 °C, and (e) $K_{13}[P_5W_{30}O_{110}K_2]$ (**2a**).

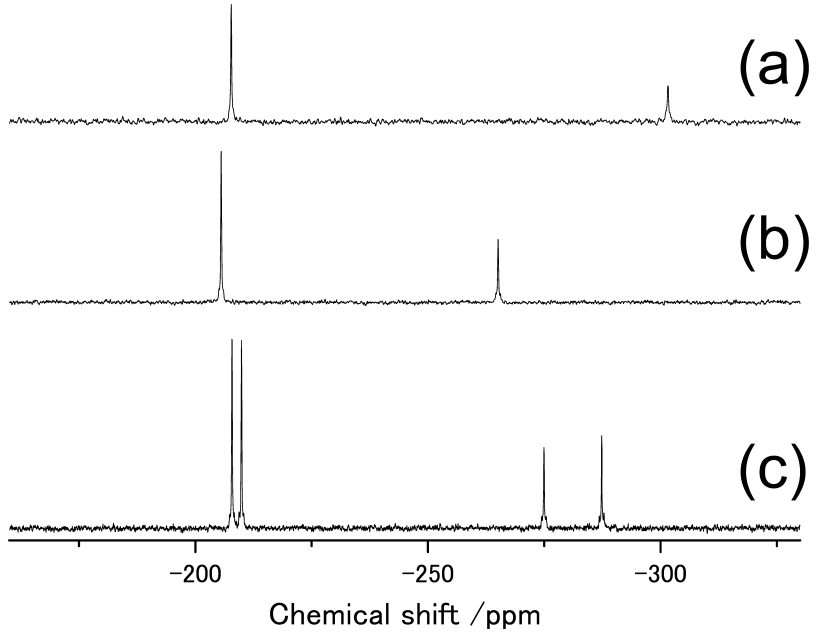

Figure 4. ^{183}W NMR spectra of (a) $K_{14}[P_5W_{30}O_{110}K]$ (**1a**), (b) $K_{13}[P_5W_{30}O_{110}K_2]$ (**2a**), and (c) $K_{14}[P_5W_{30}O_{110}Na]$. Each sample (ca. 0.5 g for **1a** and 1.0 g for $K_{13}[P_5W_{30}O_{110}K_2]$ and $K_{14}[P_5W_{30}O_{110}Na]$) was dissolved in ca. 2.5 mL of D_2O using a Li-resin.

Table 3. DFT Calculation Results

entry	most stable species	least stable species	energy diff. (kcal mol^{-1})
1	$[P_5W_{30}O_{110}K]^{14-}$ (K^+ in the central cavity) + H_2O[a]	$[P_5W_{30}O_{110}K(H_2O)]^{14-}$ (K^+ in the side cavity)[b]	35.74
2	$[P_5W_{30}O_{110}K]^{14-}$ (K^+ in the side cavity) + H_2O[a]	$[P_5W_{30}O_{110}K(H_2O)]^{14-}$ (K^+ in the side cavity)[b]	20.17
3	$[P_5W_{30}O_{110}K]^{14-}$ (K^+ in the central cavity)	$[P_5W_{30}O_{110}K]^{14-}$ (K in the side cavity)	15.6
4	$[P_5W_{30}O_{110}K_2]^{13-}$ + water molecules (K^+ in the two side cavities)	$[P_5W_{30}O_{110}K]^{14-}$ + $(K^+)_{aq}$[c] (K^+ in the central cavity)	66

[a]The H_2O molecule is outside the Preyssler molecule. [b]The H_2O molecule is inside the Preyssler molecule and coordinated to the encapsulated K^+. [c]$(K^+)_{aq}$ has been computed as a large water cluster surrounding a K^+ ion.

mers.[12,13] Thus, the structure with one K^+ cation in the side cavity may be stabilized in such a hybrid system.

Preparation and Characterization of the Acid Form $H_{14}[P_5W_{30}O_{110}K]$ (1b). Similar to other Preyssler compounds, the acid form of **1a**, $H_{14}[P_5W_{30}O_{110}K]$ (**1b**), can be prepared by the reaction of **1a** with an acidic resin (eq 1). The elemental analysis confirmed that all of the counter-cations were exchanged with protons except the encapsulated K^+, which

DOI: 10.1021/acsomega.8b00163
ACS Omega 2018, 3, 2363−2373

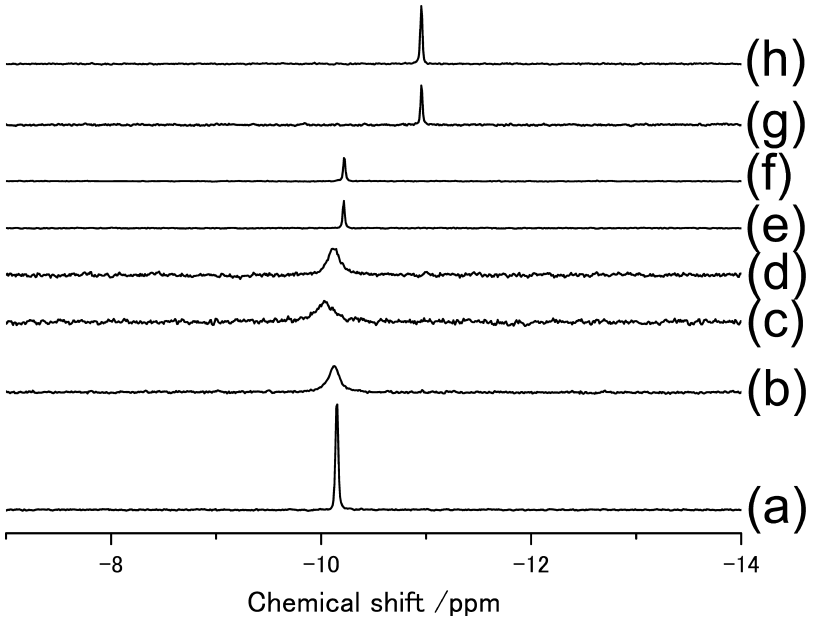

Figure 5. ^{31}P NMR spectra of $K_{14}[P_5W_{30}O_{110}K]$ (**1a**) dissolved in (a) D_2O, (c) 1 M HCl, (d) 0.1 M HCl, (e) Briton−Robinso buffer (pH 2), and (f) Briton−Robinso buffer (pH 7). ^{31}P NMR spectra of (b) $H_{14}[P_5W_{30}O_{110}K]$ (**1b**) dissolved in D_2O and of $K_{13}[P_5W_{30}O_{110}K_2]$ (**2a**) in (g) 1 M HCl and (h) D_2O. Each sample (ca. 50 mg) was dissolved in ca. 1.0 mL of solution.

was not exchanged, affording the formula $H_{14}[P_5W_{30}O_{110}K]\cdot 40H_2O$. The IR spectrum of **1b** is similar to that of **1a** in terms of the band position and sharpness (Figure 3c). These results thus confirmed the successful preparation of the acid form $H_{14}[P_5W_{30}O_{110}K]$ (**1b**) with one central K^+.

$$K_{14}[P_5W_{30}O_{110}K] + 14H^+\text{-resin} \rightarrow H_{14}[P_5W_{30}O_{110}K] + 14K^+\text{-resin} \quad (1)$$

$$H_{14}[P_5W_{30}O_{110}K] + 14KHCO_3 \rightarrow K_{14}[P_5W_{30}O_{110}K] + 7H_2O + 14CO_2 \quad (2)$$

The ^{31}P NMR spectrum of **1b** in D_2O shows one broad singlet, unusual for Preyssler-type compounds (Figure 5b), which is converted into the sharp peak of **1a** upon neutralization of **1b** with 14 equiv of $KHCO_3$ in D_2O (eq 2). It has been reported that the ^{31}P NMR spectra of Preyssler phosphotungstates, $[P_5W_{30}O_{110}M^{n+}(H_2O)]^{(15-n)-}$ ($M = Ca^{2+}$, Bi^{3+}, Eu^{3+}, Y^{3+}), show one sharp singlet or two sharp singlets depending on the pH of the solution. Pope's group has reported that the protonation of the inner oxygen of mono-cation-encapsulated Preyssler-type phosphotungstates occurs to form mono-cation-and-proton-encapsulated species (eq 3),[19] describing the pK_a value for a mono-$Eu^{3+}(H_2O)$-encapsulated compound to be below 3. We have reported the pK_a value for a mono-$Ca^{2+}(H_2O)$-encapsulated compound to be ca. 6,[18] and López and Poblet's group has reported pK_a values of less than 2 for a mono-$Na^+(H_2O)$-encapsulated compound.[23] The inner oxygens (O_a) not coordinating the encapsulated cations have been suggested to be prone to undergo such a protonation (eq 3).[19,23] The protonation−deprotonation rate is significantly slower than the NMR timescale, and thus sharp ^{31}P NMR singlets of protonated and deprotonated species are observed. Such a slow proton-exchange rate is explained by the coordination of two oxygens (one O_a not coordinating the encapsulated cation and the O of the water molecule coordinated to the encapsulated cation) to the incorporated proton. In previous paper, we reported that the potassium salt (**2a**) (Figure 5h) and acid form of the di-K^+ compound show only one sharp singlet at the same chemical shift because no protonation occurs in the cavity.[29]

$$[P_5W_{30}O_{110}M^{n+}(H_2O)]^{(15-n)-} + H^+ \rightarrow [P_5W_{30}O_{110}M^{n+}(H_2O)H]^{(14-n)-} \quad (3)$$

The ^{31}P NMR spectrum of the potassium salt **1a** became broader in an acidic solution (Figure 5c−f), indicating that the changes in the broadness of the signal are reversible. On the other hand, the ^{31}P NMR signal of **2a** in the acid solution was sharp (Figure 5g). We believe that the broad signal of **1b** in D_2O arises from the protonation−deprotonation processes of the inner oxygen, which are so fast that only one a peak is observed and whose protonation occurs at pH values lower than 2. The absence of a water molecule coordinated to the K^+ ion in **1** may be the reason why the protonation−deprotonation processes are faster than in the other Preyssler compounds.

Protonation of the inner oxygen has also been demonstrated by cyclic voltammetry (CV). It is known that the redox potentials are shifted by changing the encapsulated cation charge,[9] and the first reduction potential shifts to more positive values with the increasing charge of the incorporated cation.

The $Na^+(H_2O)$-encapsulated Preyssler-type phosphotungstate has been reported to exhibit two large redox couples and one small redox couple in 1.0 M HCl, corresponding to four-, four-, and two-electron redox processes of the tungsten atoms, respectively (Figure 6 (pink)).[9,25] The larger two, four-electron redox couples are split into two, two-electron redox couples upon exchanging Na^+ with higher-valence cations, such as Ca^{2+}, Y^{3+}, or Th^{4+}, and the first two-electron reduction potential (the most positive redox couple) is shifted to a more positive potential by increasing the cationic valence of the encapsulated cation (the first redox potentials are −0.16, −0.14, and −0.12 V vs Ag/AgCl for the $Na^+(H_2O)$-, $Ca^{2+}(H_2O)$-, and $Bi^{3+}(H_2O)$-encapsulated compounds, respectively).

DOI: 10.1021/acsomega.8b00163
ACS Omega 2018, 3, 2363−2373

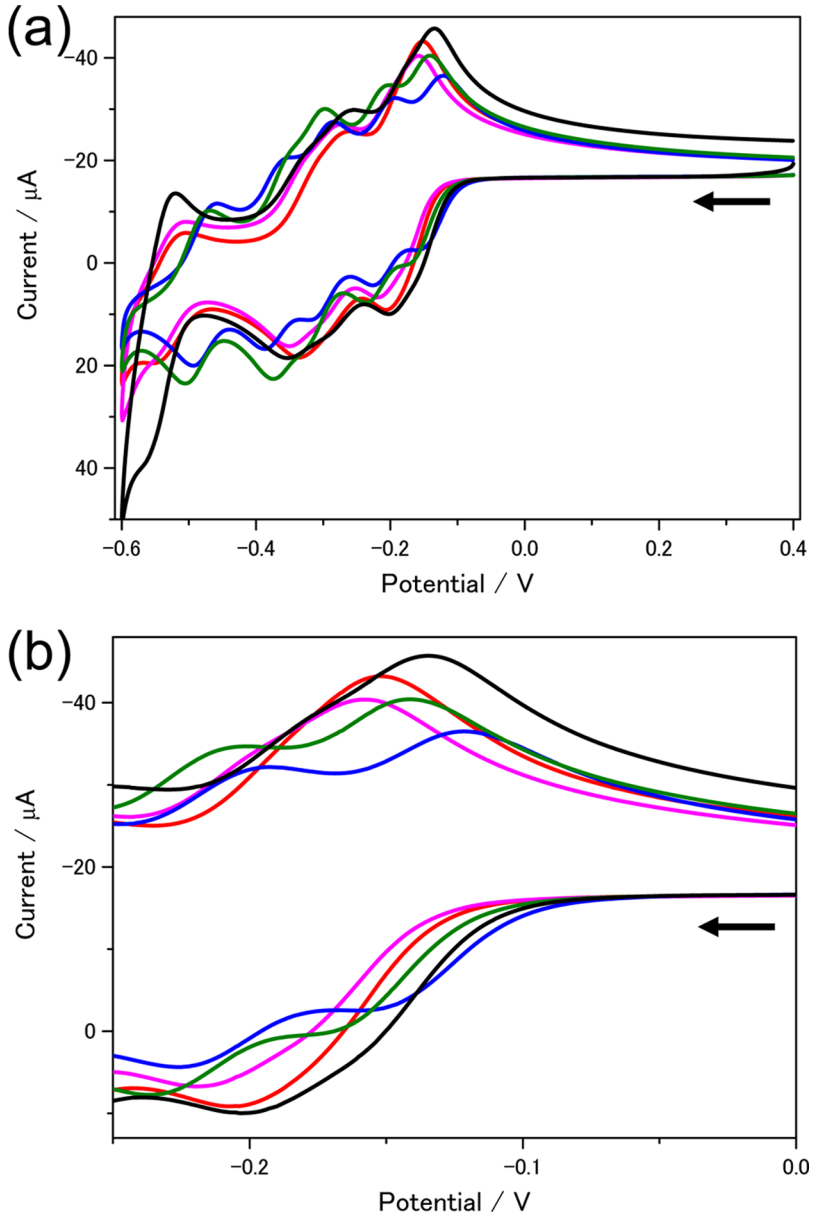

Figure 6. Cyclic voltammograms of $K_{14}[P_5W_{30}O_{110}K]$ (**1a**, black), $K_{13}[P_5W_{30}O_{110}K_2]$ (**2a**, red), $K_{14}[P_5W_{30}O_{110}Na]$ (pink), $K_{13}[P_5W_{30}O_{110}Ca]$ (green), and $K_{12}[P_5W_{30}O_{110}Bi]$ (blue). Each sample (ca. 1 mM) was dissolved in 1.0 M HCl. The arrow indicates the direction of the potential scan. (a) Potential window between 0.40 and −0.60 V. (b) An enlarged CV with potential window between 0.00 and −0.25 V.

The inner oxygen of a mono-cation-encapsulated Preyssler compounds is protonated in 1.0 M HCl,[23] and we consider that the observed redox potentials correspond to the protonated species, in which case the first reduction potential of di-K^+-encapsulated **2a** is similar to that of the $Na^+(H_2O)$-H^+-encapsulated compound.[29]

The cyclic voltammogram of **1a** in 1.0 M HCl shows three large redox couples (Figure 6a (black)). The first reduction peak current starts to increase at a more positive potential than that of **2a**, being similar to the species from the $Ca^{2+}(H_2O)$-H^+-encapsulated structure (Figure 6b), suggesting that two-proton protonation occurs in the 1.0 M HCl solution.

Reaction Conditions. To find optimal synthesis condition for mono-K^+-encapsulated species (**1**) and di-K^+-encapsulated species (**2**) under hydrothermal conditions, we varied the reaction conditions and the obtained species were analyzed by ^{31}P NMR spectroscopy (Table 1).

When $Ca^{2+}(H_2O)$-encapsulated compound $K_{13}[P_5W_{30}O_{110}Ca(H_2O)]$ was heated in KOAc buffer solution at 170 °C for 24 h, **1** and **2** were obtained in 11 and 16% yield, respectively, and the starting $Ca(H_2O)$ compound was recovered in 52% yield (entry 1). When KCl was added to the reaction solution, the conversion of the $Ca(H_2O)$ compound increased, as did the yield of **2** (entries 3, 4, 6, and 7). The conversion of the $Ca(H_2O)$ compound increased with the reaction time, the yield of **1** decreased, and that of **2** increased (entries 2 and 5). When the reaction was performed in LiOAc buffer solution, only **2** was obtained in 4% yield and the starting $Ca(H_2O)$ compound was recovered in 33% yield. In the LiOAc buffer, only a small amount of potassium (counter-cation of the starting compound) is present and able to replace the Ca^{2+} ions. These results indicate that the starting $Ca(H_2O)$ compound is consumed in the buffer solution and

DOI: 10.1021/acsomega.8b00163
ACS Omega 2018, 3, 2363−2373

the yield of both **1** and **2** increases with the increasing amount of potassium cations in the solution.

When a $Bi^{3+}(H_2O)$-encapsulated compound, $K_{12}[P_5W_{30}O_{110}Bi(H_2O)]$, was heated in the LiOAc buffer solution, **1** and **2** were obtained in 4 and 28% yield, respectively, and almost all of the starting $Bi(H_2O)$ compound was consumed (entry 9). The addition of KCl to the reaction mixture increased only the yield of **2**, whereas **1** was not detected (entries 10−12). A reaction temperature of 170 °C is required to consume the $Bi(H_2O)$ compound (entry 13) and the reaction needs to be performed in the buffer solution (entries 14 and 15).

The same reaction with a $Na^+(H_2O)$-encapsulated compound, $K_{14}[P_5W_{30}O_{110}Na(H_2O)]$, did not produce any new solids, and the Na-encapsulated compound was fully recovered (entry 16).

Thermal Conversion of Mono-K-Encapsulated Compound 1 into Di-K-Encapsulated Compound 2 in Solid State. The thermal stability of the Preyssler compounds is one of the most interesting topics for us. We have reported that the potassium salt of di-K^+-encapsulated Preyssler compound **2a** is thermally stable up to 450 °C.[29] We observed that heating of **1a** produced di-K^+-encapsulated species **2a** (Figures 3d and S2), indicating that one potassium counter-cation migrates into one of the side cavities and the K^+ in the central cavity moves into the other side cavity (Figure 7). Thermogravimetric-differential

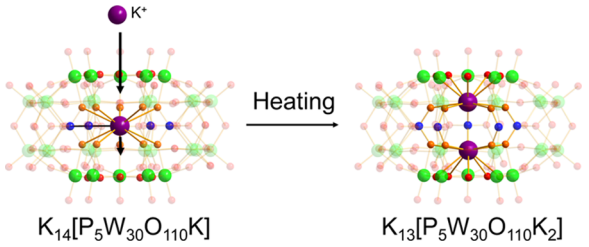

Figure 7. Schematic representation of the conversion of $K_{14}[P_5W_{30}O_{110}K]$ (**1a**) into $K_{13}[P_5W_{30}O_{110}K_2]$ (**2a**).

thermal analysis (TG-DTA) measurements of **1a** revealed an exothermal peak at a temperature between 250 and 320 °C (Figure S3), which may be assigned to the conversion of **1a** into **2a**.

Exchange of the encapsulated cations has thus been achieved under hydrothermal conditions, and this solid-state heating process offers an additional method to introduce and/or exchange the encapsulated cation in the Preyssler compounds.

Taking the mono-K^+ compound with K^+ in the center of the cavity (**1a**) as a reference, compound **2a** with two K^+ ions in the side cavities was found to be much more stable (66 kcal mol^{-1}, Table 3, entry 4). Although this process is largely exothermic, the conversion of **1a** into **2a** needs a temperature of ca. 300 °C. Intuitively, a large activation barrier must be overcome to reach the most stable product, $[P_5W_{30}O_{110}K_2]^{13-}$. The calculations show that a relatively large (thermal) energy (ca. 36−43 kcal mol^{-1}) is necessary for the cation to pass through the cavity entrance and reach the final position in the di-K structure (Figure S4).

Catalytic Activity as an Acid Catalyst. The acid form **1b** exhibits catalytic activity similar to that of other acid forms of mono-cation-encapsulated compounds toward the hydration of ethyl acetate (Table 4), and the catalytic activity per weight was found to be similar to that of the mono-$Na(H_2O)$-encapsulated compound[4] and better than that of the well-known Keggin-type phosphotungstic acid $H_3PW_{12}O_{40}$.

CONCLUSIONS

The first Preyssler-type phosphotungstate with one encapsulated potassium cation in the central cavity, $[P_5W_{30}O_{110}K]^{14-}$, was prepared as a potassium salt and characterized by empirical and theoretical methods. Heating of the potassium salt led to the migration of one potassium counter-cation into one of the side cavities, displacing the already encapsulated potassium cation to the other side cavity to form a di-K^+-encapsulated derivative. This process represents a new method to introduce cations into the Preyssler compounds.

EXPERIMENTAL SECTION

Materials. Deionized water (Millipore, Elix) was used in all of the experiments. Compounds $K_{14}[P_5W_{30}O_{110}Na(H_2O)]\cdot 23H_2O$, $K_{13}[P_5W_{30}O_{110}Ca(H_2O)]\cdot 25H_2O$, and $K_{12}[P_5W_{30}O_{110}Bi(H_2O)]\cdot 24H_2O$ were prepared according to published procedures[18] and analyzed by ^{31}P NMR and infrared (IR) spectroscopy. All of the other chemicals were reagent grade and used as supplied.

*Preparation of $K_{14}[P_5W_{30}O_{110}K]\cdot 17H_2O$ (**1a**).* $K_{13}[P_5W_{30}O_{110}Ca(H_2O)]\cdot 25H_2O$ (2.39 g, W: 9 mmol) and KCl (0.45 g, 6 mmol) were mixed in the potassium acetate buffer (2 M KOAc and 2 M AcOH mixed in a 1:1 ratio, 5 mL, pH 4.7) in a 30 mL Teflon-liner autoclave and the mixture was stirred for 5 min at room temperature. The autoclave was placed in an oven heated at 170 °C for 24 h. Once the reactor had cooled down to room temperature, the resulting colorless crystals were separated from the solution by filtration. The crystals were recrystallized from 25 mL of hot water heated at 90 °C (using a metal bath), and a final third recrystallization afforded a pure product suitable for single-crystal X-ray diffraction (XRD) analysis. The colorless crystals were collected by filtration and dried at 70 °C overnight (0.04 g, 0.005 mmol, yield of 2% based on W). Elemental anal. calcd (found) for

Table 4. Catalytic Activity for the Hydrolysis of Ethyl Acetate[a]

		rate		
catalyst	conv. (%)	per weight (mmol g^{-1} min^{-1})	per acid amount (mmol acid mol^{-1} min^{-1})	ref
$H_{14}[P_5W_{30}O_{110}Na]$	46.2	275.7	164.0	4
$H_{13}[P_5W_{30}O_{110}K_2]$	55.1	304.8	195.9	28
$H_{14}[P_5W_{30}O_{110}K]$	45.6	273.6	162.9	this work
$H_3PW_{12}O_{40}$	49.1	175.2	174.5	4
blank	1.4			4

[a]Amount of protons: 0.042 mmol, 5 wt % ethyl acetate in D_2O (total volume: 3.0 mL, ethyl acetate: 0.15 g), reaction temperature: 80 °C, reaction time: 2 h.

DOI: 10.1021/acsomega.8b00163
ACS Omega 2018, 3, 2363−2373

$K_{14}[P_5W_{30}O_{110}K]\cdot 17H_2O$ (%): P, 1.86 (1.85); W, 66.3 (66.4); K, 7.05 (7.11); H, 0.48 (0.46).

*Preparation of $H_{14}[P_5W_{30}O_{110}K]\cdot 40H_2O$ (**1b**).* $K_{14}[P_5W_{30}O_{110}K]\cdot 17H_2O$ (0.20 g) was dissolved in H_2O (8 mL) and passed through 2.5 g of Dowex 50 WX8 in a protonic form packed in a glass tube (inner diameter: 20 mm) with additional water until the eluent was neutral. The eluent was then evaporated using a rotary evaporator in vacuo at 60 °C. A minimum amount of water was added, and the resulting solution was poured into a glass beaker and dried at 70 °C overnight (0.18 g, 0.13 mmol, yield of 93% based on W). Elemental anal. calcd (found) for $H_{14}[P_5W_{30}O_{110}K]\cdot 40H_2O$ (%): P, 1.89 (1.88); W, 67.2 (67.2); K, 0.485 (0.51); H, 1.06 (1.161).

X-ray Crystallography. Single-crystal X-ray diffraction (XRD) data for the **1a** crystals were collected on a Bruker SMART APEX II ULTRA diffractometer at 173 K using a monochromated Mo Kα radiation (λ = 0.71073 Å). The structure was solved via direct methods using a SHELXS-97 and refined via the full-matrix least-squares method on F^2 with SHELXL-97.[31] The atoms of the polyoxometalate molecules and counter-cations were refined anisotropically, and the oxygen atoms of crystalline water molecules were located in a difference Fourier map and refined with isotropic thermal parameters. The hydrogen atoms of crystalline water were not located. The number of potassium atoms and water oxygen atoms determined by XRD was lesser than that determined by elemental analysis due to disorder in the structure. The crystallographic data are summarized in Table 5. Further details

Table 5. Crystal Data of $K_{14}[P_5W_{30}O_{110}K]$ (1a)

compound	$K_{14}[P_5W_{30}O_{110}K]\cdot 17H_2O$
empirical formula	$K_{15}P_5W_{30}O_{127}H_{34}$
molecular weight/g mol^{-1}	7981.28
crystal size/mm	0.10 × 0.10 × 0.08
crystal color and shape	colorless, block
temperature/K	173
crystal system	orthorhombic
space group (no.)	*Pnna* (52)
a/Å	32.6621(15)
b/Å	21.5252(10)
c/Å	19.0566(9)
volume/Å^3	13 397.9(11)
Z	4
data/parameters	15 370/901
R (int)	0.0245
density (calcd)/g cm^{-1}	4.249
abs. coefficient/mm^{-1}	26.220
R_1 ($I > 2s(I)$)[a]	0.0229
wR_2 (all data)[b]	0.0522

[a] $R_1 = \sum||F_o| - |F_c||/\sum|F_o|$. [b] $R_w = [\sum w(F_o^2 - F_c^2)^2]/\sum[w(F_o^2)^2]^{1/2}$.

of the crystal structure analysis can be obtained from Fachinformationszentrum Karlsruhe, 76344 Eggenstein-Leopoldshafen, Germany (fax: +49-7247-808-666; e-mail: crysdata@fiz-karlsruhe.de); http://www.fiz-karlsruhe.de/request_for_deposited_data.html on quoting the deposition number CSD-433840 for $K_{14}[P_5W_{30}O_{110}K]$ (**1a**).

Other Analytical Techniques. The IR spectra were recorded on a NICOLET 6700 Fourier transform infrared spectrometer (Thermo Fisher Scientific) as KBr pellets. The cyclic voltammetry (CV) was performed on a CHI620D system (BAS Inc.) at ambient temperature. A glassy carbon working electrode (diameter, 3 mm), a platinum wire counter electrode, and an Ag/AgCl reference electrode (203 mV vs the normal hydrogen electrode at 25 °C) (3 M NaCl, BAS Inc.) were used. The approximate formal potential values ($E_{1/2}$ values) were calculated from the CVs as the average of the cathodic and anodic peak potentials for the corresponding oxidation and reduction waves. The ^{31}P NMR spectra were recorded on a Varian 500 (500 MHz) spectrometer (Agilent, P resonance frequency: 202.333 MHz). The spectra were referenced to external 85% H_3PO_4 (0 ppm). The ^{183}W NMR spectra were recorded on a Varian 500 (500 MHz) spectrometer (Agilent) (W resonance frequency: 20.825 MHz). The spectra were referenced to an external saturated Na_2WO_4 (0 ppm). The **1a** sample for ^{183}W NMR spectroscopy was treated with lithium resin to increase its solubility in D_2O. Elemental analyses were carried out by Mikroanalytisches Labor Pascher (Remagen, Germany). High-resolution ESI-MS spectra were recorded on an LTQ Orbitrap XL instrument (Thermo Fisher Scientific) with an accuracy of 3 ppm. Each sample (5 mg) was dissolved in 5 mL of H_2O, and the solutions were diluted with CH_3CN (final concentration: ca. 10 μg mL^{-1}).

Hydrolysis of Ethyl Acetate. Hydrolysis of ethyl acetate was carried out at 80 °C with 5 wt % ethyl acetate in D_2O (total volume: 3.0 mL, ethyl acetate: 0.15 g) for 2 h.[4] The amount of protons used was maintained at 0.042 mmol.

Electronic Structure Calculations. Density functional theory (DFT) calculations were performed for the $[P_5W_{30}O_{110}K]^{14-}$, $[P_5W_{30}O_{110}K(H_2O)]^{14-}$, and $[P_5W_{30}O_{110}K_2]^{13-}$ structures with the ADF 2016 suite of programs.[32,33] Intermediate geometries were also analyzed to estimate the K^+ encapsulation energy profile. Equilibrium geometries were obtained upon full geometry optimization with tight convergence criteria (optimized structures must be very accurate when frequency calculations are to be conducted because molecular vibrations can be highly dependent on the geometrical parameters) and the OPBE functional[34,35] with triple-ζ + double polarization atomic basis sets, using the frozen core approximation for the following shells: 1s−3p for K, 1s−2p for P, 1s−4f for W, and 1s for O. We simulated an aqueous solution (dielectric constant, ε = 78.39) by including the solvent and counterion effects by means of the conductor-like screening model.[36−39]

■ ASSOCIATED CONTENT

Supporting Information

The Supporting Information is available free of charge on the ACS Publications website at DOI: 10.1021/acsomega.8b00163.

ESI-MS spectra of **1a** (Figure S1); ^{31}P NMR and IR spectra of the heated samples of **1a** (Figure S2); TG-DTA curves of **1a** and **2a** (Figure S3); energy profile for the encapsulation of a K^+ ion (Figure S4); optimized structures by DFT (Table S1) (PDF)

Crystallographic data (CIF)

■ AUTHOR INFORMATION

Corresponding Author

*E-mail: sadakane09@hiroshima-u.ac.jp. Tel: +81 82 424 4456. Fax: +81 82 424 5494.

ORCID

Masahiro Sadakane: 0000-0001-7308-563X

Notes

The authors declare no competing financial interest.

DOI: 10.1021/acsomega.8b00163
ACS Omega 2018, 3, 2363−2373

■ ACKNOWLEDGMENTS

M.S. is grateful for the A-STEP program of the Japanese Science and Technology Agency (JST), and Furukawa Foundation for the Promotion of Technology. X.L. thanks the Spanish Ministry of Science and Innovation (MICINN) (project CTQ2011-29054-C02-01/BQU), the DGR of the Generalitat de Catalunya (grant no. 2014SGR199), and the XRQTC. This work was also supported by the Center for Functional Nano Oxide at Hiroshima University. M.N.K.W. thanks the Indonesian Endowment Fund for Education (LPDP), Ministry of Finance, Republik Indonesia, for a Ph.D. scholarship. We thank T. Amimoto and N. Kawata at the Natural Science Center for Basic Research and Development (N-BARD), Hiroshima University, for the ESI-MS measurements and the initial single-crystal X-ray structure analysis, respectively.

■ REFERENCES

(1) Pope, M. T. *Heteropoly and Isopoly Oxometalates*; Springer-Verlag: Berlin, 1983; pp 1−196.
(2) Hill, C. L. Thematic issue on Polyoxometalates. *Chem. Rev.* **1998**, *98*, 1−390.
(3) Cronin, L.; Müller, A. Thematic Issue on Polyoxometalates. *Chem. Soc. Rev.* **2012**, *41*, 7333−7334.
(4) Sadakane, M.; Ichi, Y.; Ide, Y.; Sano, T. Thermal Stability and Acidic Strength of Preyssler-Type Phosphotungstic Acid, $H_{14}[P_5W_{30}O_{110}Na]$ and It's Catalytic Activity for Hydrolysis of Alkyl Acetates. *Z. Anorg. Allg. Chem.* **2011**, *637*, 2120−2124.
(5) Du, J.; Cao, M.-D.; Feng, S.-L.; Su, F.; Sang, X.-J.; Zhang, L.-C.; You, W.-S.; Yang, M.; Zhu, Z.-M. Two New Preyssler-Type Polyoxometalate-Based Coordination Polymers and Their Application in Horseradish Peroxidase Immobilization. *Chem. − Eur. J.* **2017**, *23*, 14614−14622.
(6) Kobayashi, D.; Ouchi, Y.; Sadakane, M.; Unoura, K.; Nabika, H. Structural Dependence of the Effects of Polyoxometalates on Liposome Collapse Activity. *Chem. Lett.* **2017**, *46*, 533−535.
(7) Niinomi, K.; Miyazawa, S.; Hibino, M.; Mizuno, N.; Uchida, S. High Proton Conduction in Crystalline Composites Based on Preyssler-Type Polyoxometalates and Polymers under Nonhumidified or Humidified Conditions. *Inorg. Chem.* **2017**, *56*, 15187−15193.
(8) Alizadeh, M. H.; Harmalker, S. P.; Jeannin, Y.; Martin-Frère, J.; Pope, M. T. A Heteropolyanion with Fivefold Molecular Symmetry That Contains a Nonlabile Encapsulated Sodium Ion. The Structure and Chemistry of $[NaP_5W_{30}O_{110}]^{14-}$. *J. Am. Chem. Soc.* **1985**, *107*, 2662−2669.
(9) Creaser, I.; Heckel, M. C.; Neitz, R. J.; Pope, M. T. Rigid Nonlabile Polyoxometalate Cryptates $[ZP_5W_{30}O_{110}]^{(15-n)-}$ That Exhibit Unprecedented Selectivity for Certain Lanthanide and Other Multivalent Cations. *Inorg. Chem.* **1993**, *32*, 1573−1578.
(10) Liang, M.-X.; Ruan, C.-Z.; Sun, D.; Kong, X.-J.; Ren, Y.-P.; Long, L.-S.; Huang, R.-B.; Zheng, L.-S. Solvothermal Synthesis of Four Polyoxometalate-Based Coordination Polymers Including Diverse Ag(I)···π Interactions. *Inorg. Chem.* **2014**, *53*, 897−902.
(11) Kato, C.; Maryunina, K. Y.; Inoue, K.; Yamaguchi, S.; Miyaoka, H.; Hayashi, A.; Sadakane, M.; Tsunashima, R.; Nishihara, S. Synthesis, Characterization, and Structure of a Reduced Preyssler-type Polyoxometalate. *Chem. Lett.* **2017**, *46*, 602−604.
(12) Hu, T.-P.; Zhao, Y.-Q.; Jagličić, Z.; Yu, K.; Wang, X.-P.; Sun, D. Four Hybrid Materials Based on Preyssler P_5W_{30} Polyoxometalate and First-Row Transition-Metal Complex. *Inorg. Chem.* **2015**, *54*, 7415−7423.
(13) Zhao, Y.-Q.; Yu, K.; Wang, L.-W.; Wang, Y.; Wang, X.-P.; Sun, D. Anion-Induced Supramolecular Isomerism in Two Preyssler P_5W_{30} Polyoxometalate-Based Hybrid Materials. *Inorg. Chem.* **2014**, *53*, 11046−11050.
(14) Dickman, M. H.; Gama, G. J.; Kim, K.-C.; Pope, M. T. The Structures of Europium(III)- and Uranium(IV) Derivatives of $[P_5W_{30}O_{110}]^{15-}$: Evidence for "Cryptohydration". *J. Cluster Sci.* **1996**, *7*, 567−583.
(15) Williams, C. W.; Antonio, M. R.; Soderholm, L. The formation and stability of $[EuP_5W_{30}O_{110}]^{12-}$ and $[AmP_5W_{30}O_{110}]^{12-}$. *J. Alloys Compd.* **2000**, *303*−*304*, 509−513.
(16) Antonio, M. R.; Soderholm, L. Cerium Valence in Cerium-Exchanged Preyssler's Heteropolyanion through X-ray Absorption Near-Edge Structure. *Inorg. Chem.* **1994**, *33*, 5988−5993.
(17) Granadeiro, C. M.; de Castro, B.; Balula, S. S.; Cunha-Silva, L. Lanthanopolyoxometalates: From the structure of polyanions to the design of functional materials. *Polyhedron* **2013**, *52*, 10−24.
(18) Takahashi, K.; Sano, T.; Sadakane, M. Preparation and characterization of Preyssler-type Phosphotungstic Acid, $H_{15-n}[P_5W_{30}O_{110}M^{n+}]$, with Different Encapsulated Cations (M = Na, Ca, Bi, Eu, Y, or Ce), and their Thermal Stability and Acid Catalyst Properties. *Z. Anorg. Allg. Chem.* **2014**, *640*, 1314−1321.
(19) Kim, K.-C.; Pope, M. T.; Gama, G. J.; Dickman, M. H. Slow Proton Exchange in Aqueous Solution. Consequences of Protonation and Hydration within the Central Cavity of Preyssler Anion Derivatives, $[lM(H_2O)lP_5W_{30}O_{110}]^{n-}$. *J. Am. Chem. Soc.* **1999**, *121*, 11164−11170.
(20) Hayashi, A.; Haioka, T.; Takahashi, K.; Bassil, B. S.; Kortz, U.; Sano, T.; Sadakane, M. Cation Effect on Formation of Preyssler-type 30-Tungsto-5-phosphate: Enhanced Yield of Na-encapsulated Derivative and Direct Synthesis of Ca- and Bi-Encapsulated Derivatives. *Z. Anorg. Allg. Chem.* **2015**, *641*, 2670−2676.
(21) Antonio, M. R.; Chiang, M.-H. Stabilization of Plutonium(III) in the Preyssler Polyoxometalate. *Inorg. Chem.* **2008**, *47*, 8278−8285.
(22) Cardona-Serra, S.; Clemente-Juan, J. M.; Coronado, E.; Gaita-Ariño, A.; Camón, A.; Evangelisti, M.; Luis, F.; Martínes-Pérez, M. J.; Sesé, J. Lanthanoid Single-Ion Magnets Based on Polyoxometalates with a 5-fold Symmetry: The Series $[LnP_5W_{30}O_{110}]^{12-}$ (Ln^{3+} = Tb, Dy, Ho, Er, Tm, and Yb). *J. Am. Chem. Soc.* **2012**, *134*, 14982−14990.
(23) Fernández, J. A.; López, X.; Bo, C.; de Graaf, C.; Baerends, E. J.; Poblet, J. M. Polyoxometalates with Internal Cavities: Redox Activity, Basicity, and Cation Encapsulation in $[X^{n+}P_5W_{30}O_{110}]^{(15-n)-}$ Preyssler Complexes, with X = Na^+, Ca^{2+}, Y^{3+}, La^{3+}, Ce^{3+}, and Th^{4+}. *J. Am. Chem. Soc.* **2007**, *129*, 12244−12253.
(24) Antonio, M. R.; Soderholm, L. Implications of the unusual redox behavior exhibited by the heteropolyanion $[EuP_5W_{30}O_{110}]^{12-}$. *J. Alloys Compd.* **1997**, *250*, 541−543.
(25) Chiang, M.-H.; Antonio, M. R.; Williams, C. W.; Soderholm, L. A unique coordination environment for an ion: EXAFS studies and bond valence model approach of the encapsulated cation in the Preyssler anion. *Dalton Trans.* **2004**, 801−806.
(26) Soderholm, L.; Liu, G. K.; Muntean, J.; Malinsky, J.; Antonio, M. R. Coordination and Valence of Europium in the Heteropolyanion $[EuP_5W_{30}O_{110}]^{12-}$. *J. Phys. Chem.* **1995**, *99*, 9611−9616.
(27) Antonio, M. R.; Soderholm, L. Redox Behavior of Europium in the Preyssler Heteropolyanion $[EuP_5W_{30}O_{110}]^{12-}$. *J. Cluster Sci.* **1996**, *7*, 585−591.
(28) Antonio, M. R.; Soderholm, L.; Williams, C. W.; Ullah, N.; Francesconi, L. C. Redox behavior of cerium in heteropolyoxotungstate complexes. *J. Chem. Soc., Dalton Trans.* **1999**, 3825−3830.
(29) Hayashi, A.; Ota, H.; López, X.; Hiyoshi, N.; Tsunoji, N.; Sano, T.; Sadakane, M. Encapsulation of Two Potassium Cations in Preyssler-Type Phosphotungstates: Preparation, Structural Characterization, Thermal Stability, Activity as an Acid Catalyst, and HAADF-STEM Images. *Inorg. Chem.* **2016**, *55*, 11583−11592.
(30) Zhang, Z.-M.; Yao, S.; Li, Y.-G.; Han, X.-B.; Su, Z.-M.; Wang, Z.-S.; Wang, E.-B. Inorganic Crown Ethers: Sulfate-Based Preyssler Polyoxometalates. *Chem. − Eur. J.* **2012**, *18*, 9184−9188.
(31) Sheldrick, G. M. A short history of SHELX. *Acta Crystallogr., A* **2008**, *A64*, 112−122.
(32) Guerra, C. F.; Snijders, J. G.; te Velde, G.; Baerends, E. J. Towards an order-N DFT method. *Theor. Chem. Acc.* **1998**, *99*, 391−403.

DOI: 10.1021/acsomega.8b00163
ACS Omega 2018, 3, 2363−2373

(33) te Velde, G.; Bickelhaupt, F. M.; van Gisbergen, S. J. A.; Guerra, C. F.; Baerends, E. J.; Snijders, J. G.; Ziegler, T. Chemistry with ADF. *J. Comput. Chem.* **2001**, *22*, 931−967.
(34) Handy, N. C.; Cohen, A. J. Left-right correlation energy. *Mol. Phys.* **2001**, *99*, 403−412.
(35) Swart, M.; Ehler, A. W.; Lammertsma, K. Performance of the OPBE exchange-correlation functional. *Mol. Phys.* **2004**, *102*, 2467−2474.
(36) Klamt, A.; Schüürmann, G. COSMO: A New Approach to Dielectric Screening in Solvents with Explicit Expressions for the Screening Energy and its Gradient. *J. Chem. Soc., Perkin Trans. 2* **1993**, 799−805.
(37) Andzelm, J.; Kölmel, C.; Klamt, A. Incorporation of solvent effects into density functional calculations of molecular energies and geometries. *J. Chem. Phys.* **1995**, *103*, 9312−9320.
(38) Klamt, A. Conductor-like Screening Model for Real Solvents: A New Approach to the Quantitative Calculation of Solvation Phenomena. *J. Phys. Chem.* **1995**, *99*, 2224−2235.
(39) Pye, C. C.; Ziegler, T. An implementation of the conductor-like screening model of solvation within the Amsterdam density functional package. *Theor. Chem. Acc.* **1999**, *101*, 396−408.

DOI: 10.1021/acsomega.8b00163
ACS Omega 2018, 3, 2363−2373